

# Bloch Surface Wave-Assisted Ultrafast All-Optical Switching in Graphene

Anna A. Popkova, Aleksandr A. Chezhegov, Maxim G. Rybin, Irina V. Soboleva, Elena D. Obratsova, Vladimir O. Bessonov, and Andrey A. Fedyanin\*

Graphene has ultrafast charge carrier dynamic and shows strong light–matter interaction allowing the use in photovoltaic devices, fast photodetectors, saturable absorbers, and electro-optical modulators. However, despite the high nonlinear optical susceptibilities, the small amount of material significantly limits the use of graphene for nonlinear optical applications. In this work, Bloch surface waves (BSWs) are employed, enhancing the graphene–light interaction, for all-optical switching realization. By placing a graphene monolayer on top of a 1D photonic crystal, it is shown that for the wavelength corresponding to the BSW resonance, the reflection coefficient is modulated on the sub-picosecond time scale by an order of magnitude larger than that for bare graphene. The magnitude of the reflection change reaches 0.3% at the fluence of  $40 \mu\text{J cm}^{-2}$ . The reported results are proof of principle possibility of BSW-assisted enhancing the reflection modulation of any 2D materials and transparent thin films while maintaining their inherent ultrafast dynamics, which is useful for the further development of all-optical switches.

a giant third-order nonlinear optical susceptibility<sup>[1]</sup> in the visible and near-IR spectral ranges due to 2D electronic system, very high charge carrier mobility and strong light–matter interaction.<sup>[2,3]</sup> At this moment, the use of graphene in photovoltaic modules,<sup>[4]</sup> fast photodetectors,<sup>[5]</sup> saturable absorbers<sup>[6–8]</sup> and electro-optical modulators<sup>[9]</sup> have been demonstrated. However, the optical modulation effects in graphene are small due to the small amount of material,<sup>[10,11]</sup> and more complicated approaches are required to realize the all-optical switching. The efficiency of nonlinear optical effects can be amplified by enhancing the light–material interaction via excitation of 2D surface waves. These effects have been demonstrated in plasmonic systems<sup>[12]</sup> including graphene,<sup>[13–15]</sup> as well as in photonic systems supporting Tamm plasmons.<sup>[16]</sup>

## 1. Introduction

One of the most important tasks of modern photonics is creating ultrafast active elements which can be the basis of photonic technologies. To control the light, it is necessary to use materials with large cubic nonlinear susceptibilities. Possible candidates are 2D materials showing an increase in nonlinear effects efficiencies in comparison with their 3D counterparts, that together with the extremely small thickness allows creating flat miniature optoelectronic and optical devices. Graphene has

Here Bloch surface waves (BSWs) are used as 2D electromagnetic waves. These optical states can be excited in a completely dielectric medium, in particular, at the interface between 1D photonic crystals (PCs) and dielectrics<sup>[17,18]</sup> and reveal themselves as the narrow spectral-angular resonances in reflectance whose quality factor reach the values up to  $10^4$ .<sup>[19]</sup> Unique BSW properties including sensitive spectral-angular resonance,<sup>[20]</sup> localization of the electromagnetic field near the surface<sup>[21]</sup> and long propagation length of several millimeters<sup>[22]</sup> are in demand for many applications such as sensing,<sup>[18]</sup> micromanipulation,<sup>[23]</sup> enhancement of magneto-optical<sup>[24]</sup> and nonlinear-optical<sup>[25]</sup> effects, as well as for integrated optical applications.<sup>[26–29]</sup> Placing 2D materials on the PC surface near the maximum of the electromagnetic field makes it possible to enhance significantly the observed effects.<sup>[30]</sup> Thus, an increase in absorption,<sup>[31,32]</sup> and Goos-Hänchen shift<sup>[33]</sup> were shown when graphene was put on the PC surface. The possibility of excitation of surface electromagnetic waves in a graphene-based Bragg grating was also observed.<sup>[34]</sup>


In this article, we demonstrate how the excitation of BSWs enhances the ultrafast optical reflection modulation in graphene monolayer. We study experimentally a temporal reflectance of PC covered with a graphene monolayer. The BSW resonance sensitivity to the parameters of the medium adjacent to the PC surface allows us to increase significantly the modulation of the graphene reflection due to the shape modification and spectral shift of the resonance. Using pump-probe

A. A. Popkova, A. A. Chezhegov, I. V. Soboleva, V. O. Bessonov, A. A. Fedyanin

Faculty of Physics  
 Lomonosov Moscow State University  
 Moscow 119991, Russia  
 E-mail: fedyanin@nanolab.phys.msu.ru

M. G. Rybin, E. D. Obratsova  
 Prokhorov General Physics Institute  
 Russian Academy of Sciences  
 Moscow 119991, Russia

I. V. Soboleva, V. O. Bessonov  
 Frumkin Institute of Physical Chemistry and Electrochemistry  
 Russian Academy of Sciences  
 Moscow 119071, Russia

 The ORCID identification number(s) for the author(s) of this article can be found under <https://doi.org/10.1002/adom.202101937>.

DOI: 10.1002/adom.202101937

technique in Kretschmann prism configuration,<sup>[35]</sup> we observe that the reflectance modulation strongly intensifies at the probe wavelength near the BSW resonance. The modulation of an order of magnitude greater than that for graphene on a conventional substrate is obtained for near-infrared spectral region at a quite low pump fluence of  $40 \mu\text{J cm}^{-2}$ .

## 2. Results and Discussion

The sample is a 1D photonic crystal consisted of 7 pairs of alternating quarter-wavelength-thick layers of  $\text{SiO}_2$  and  $\text{Ta}_2\text{O}_5$  deposited on a fused quartz substrate. PC layer thicknesses are optimized for BSW excitation in the Kretschmann scheme for the TE-polarized radiation at the wavelength of 800 nm and the incident angle of  $45^\circ$ . A graphene monolayer is prepared by chemical vapor deposition method<sup>[36]</sup> and transferred at the PC surface using wet transfer by polymethyl methacrylate.<sup>[37]</sup> A bare PC surface is used as a reference. The detailed information on the sample parameters, their optimization and PC preparation is given in Section S1, Supporting Information.

Measurements of the transient reflectance are performed by cross-polarization pump-probe technique combined with the Kretschmann prism configuration. As a light source we use a Ti:sapphire femtosecond laser (Coherent Micra) generating pulses with spectral width at half maximum of 30 nm and pulse duration of 50 fs. Schematic outline of the experiment is shown in **Figure 1a**. The pump beam is focused on the PC/graphene interface at the normal incidence into a  $50 \mu\text{m}$  spot, while the probe beam is focused at the same point at the  $45^\circ$ -incidence through a right-angle prism and PC substrate. The probe focal spot on the PC surface is elliptical with axis sizes of 20 and  $30 \mu\text{m}$ . A part of the probe radiation excites BSW propagating along the PC/graphene interface, that yields a narrow absorption resonance in the spectrum of the reflected probe pulse measured with a monochromator and a photomultiplier tube (PMT). The synchronous detection system allows us to detect the ultrafast reflection modulation at the same time. Under the pump radiation, the complex permittivity of the graphene monolayer is modulated at subpicosecond time scale

leading to variation in the quality factor and the wavelength of the BSW resonance. This results in an increased modulation of the reflection coefficient at certain wavelengths close to the BSW resonance. We also visualize the sample surface to observe the BSW excitation and propagation (**Figure 1b**). The detailed description of the experimental setup is given in Section S2, Supporting Information.

First, we measure the spectra of unfocused probe pulses reflected from the bare PC and PC/graphene samples to determine the BSW resonance properties (**Figure 2a,b insets**). Then, the spectra were normalized by the probe pulse spectrum obtained in the same conditions (Kretschmann scheme,  $45^\circ$  incident angle) for a bare substrate. The resulted reflectance spectra shown in **Figure 2a** demonstrate the sharp resonance at the wavelength of 782 nm revealing the BSW excitation. When a graphene monolayer, which has a significant absorption and a sufficiently large refractive index,<sup>[38]</sup> is placed at the PC surface, the resonance widens and shifts to the long-wave region of the spectrum towards 785 nm. The Q-factors of the BSW resonances are estimated to be  $375 \pm 5$  and  $110 \pm 10$  for bare PC and PC/graphene, respectively. The effect of absorption is also seen in **Figure 1b** as shortening the propagation length of BSW in the graphene monolayer.

The pump-probe scheme requires focusing a laser beam on the sample surface to increase the light intensity, which in conjunction with the use of wide-spectrum laser pulses provides the multiple BSWs excitation at various wavelengths and incidence angles in accordance with the BSW dispersion law.<sup>[39]</sup> In this case, the high-Q BSW resonance can not be observed in the reflection spectrum, since it is integrated over the spectral and angular components of the probe radiation (see **Figure 2c,d**). The Q-factors of the BSW resonances decrease to  $110 \pm 10$  and  $85 \pm 5$  for bare PC and PC/graphene, respectively. To minimize this effect we implement a spatial filter consisted of a lens and an aperture. The probe radiation reflected from the sample is collected by the lens with the focal length of 200 mm. The aperture with the 1-mm diameter is placed at the back focal plane of the lens, where different points of the focus plane correspond to different reflected angles of the probe. The system selects the reflected beams corresponding to a set of incident angles with  $\text{NA} = 0.0025$ . The spectra obtained with the spatial filter for the focused probe beam are shown in **Figure 2e,f**. The corresponding Q-factors of the BSW resonances are increased to  $175 \pm 5$  and  $90 \pm 5$ , but remain smaller than the values for the unfocused case. This is due to a slight averaging over the spectral positions of the BSW resonance in accordance with the range of filtered angles of incidence.

The time-resolved reflectance spectroscopy of the PC/graphene sample is performed at the pump fluence of  $40 \mu\text{J cm}^{-2}$  to provide the highest signal level without damage of graphene. The probe fluence of  $5 \mu\text{J cm}^{-2}$  is chosen to minimize its influence on the graphene optical constants (see Section S3, Supporting Information for details). The linear polarizations of pump and probe beams are orthogonal in all pump-probe experiments. **Figure 3a** shows the relative change in the sample reflectance,  $\Delta R/R$ , measured for the TE-polarized probe radiation as a function of probe wavelength and time delay between the pump and probe pulses. The wavelength dependence of  $\Delta R/R$  reveals sharp resonance at 785 nm reaching the maximum value of 0.3%. The experimental data perfectly fits

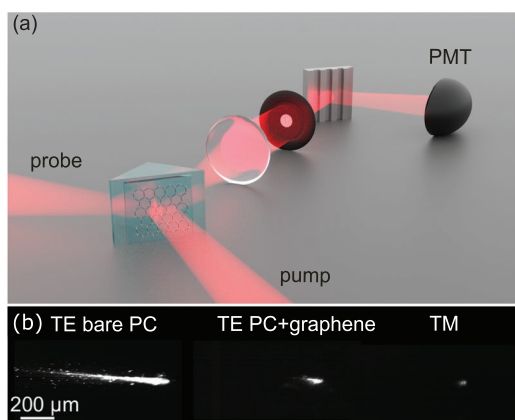


**Figure 1.** a) Sketch of the experiment. b) The images of surfaces of PC and PC/graphene samples for TE polarization of probe beam and TM ones from left to right.

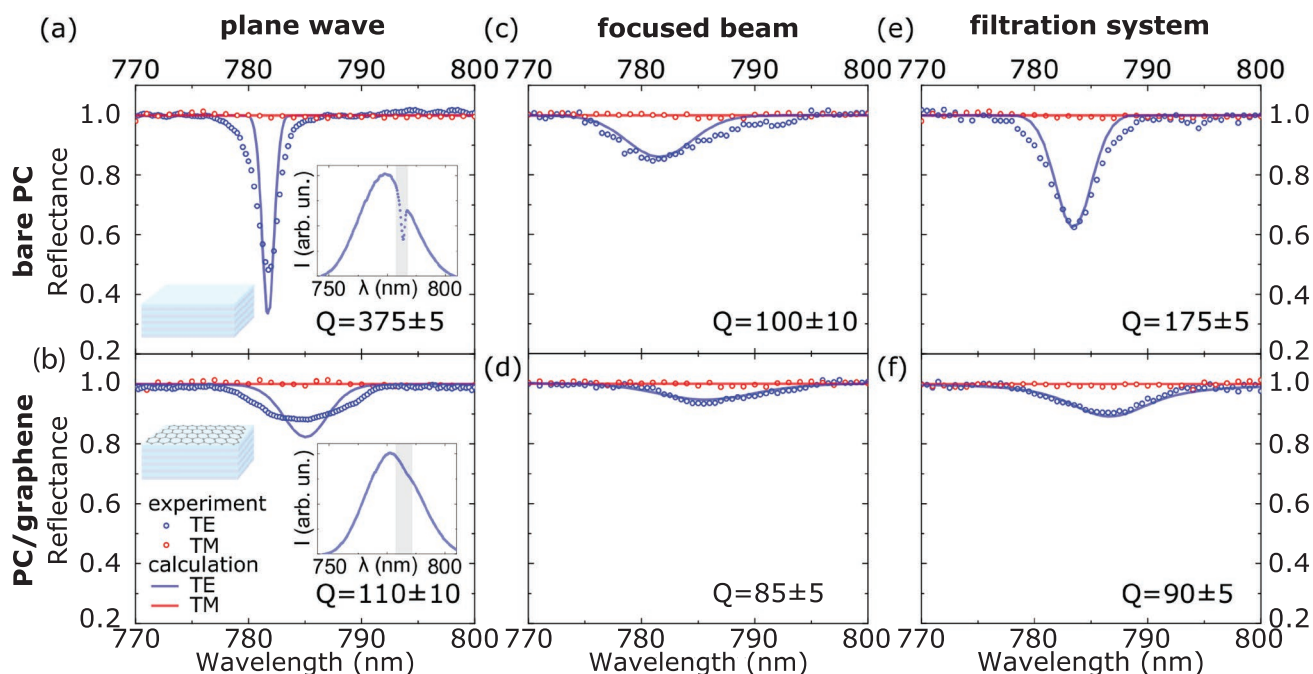


**Figure 2.** Reflectance spectra of PC (top) and PC/graphene (bottom) samples for a,b) plane wave illumination, using c,d) focused beam and e,f) filtration system. Inserts show the raw spectra of reflected pulses. The BSW resonance regions are highlighted with gray areas.

to the numerical simulations (Figure 3b), the details of which are discussed below. Figure 3c shows the cross-section of the time-resolved spectrum for the 200-fs delay and the reflectance spectrum of the PC/graphene sample. The  $\Delta R/R$  resonance matches with the BSW resonance in reflectance of the sample.

The time-resolved  $\Delta R/R$  spectra for TM-polarized probe radiation shown in Figure 3d are featureless and show non-zero  $\Delta R/R$  values only near the zero delay. The maximum  $\Delta R/R$  value is 0.07% at 785 nm wavelength and 200 fs delay, which is five times smaller than in the case of BSW excitation. The

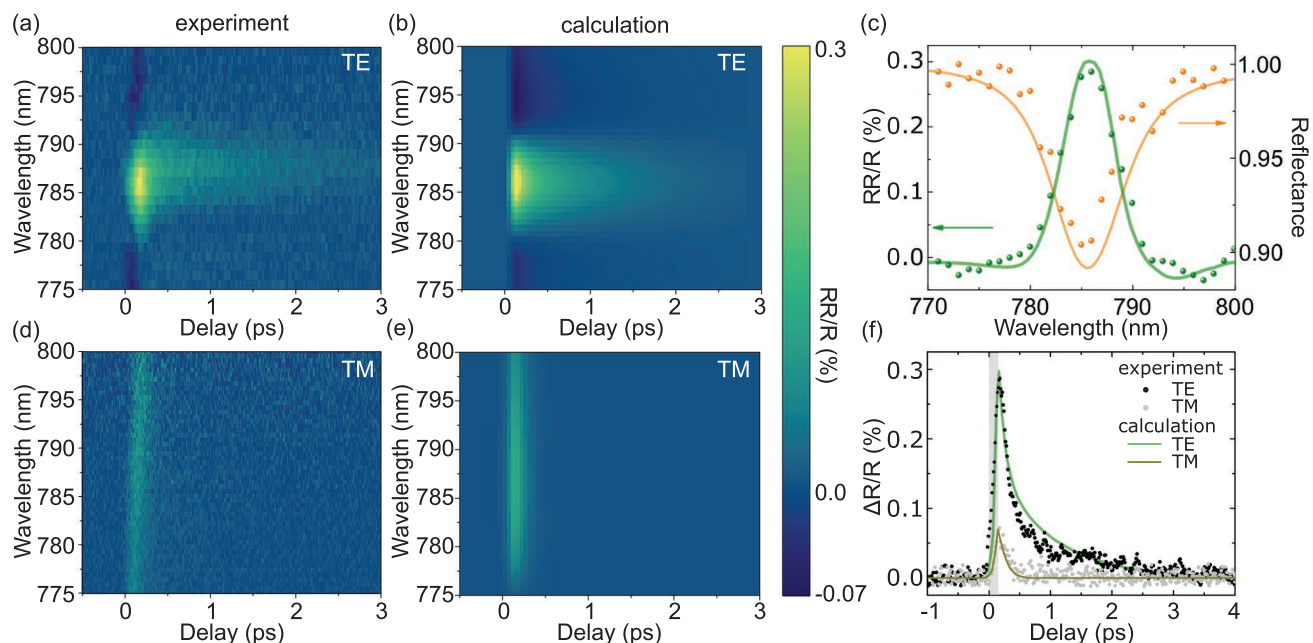


**Figure 3.** a,b) Measured and calculated time-resolved spectral dependences of reflectance modulation for the TE-polarized probe. c) Spectral dependences of PC/graphene reflectance (orange) and  $\Delta R/R$  (green) for 200 fs delay corresponding to the maximum of modulation. Solid curves are numerical calculations. d,e) Measured and calculated time-resolved spectral dependences for TM probe polarization. f) Transient reflectance for the 785 nm wavelength corresponding to the BSW resonance.

observed modulation of the reflection is due to changes in the optical constants of graphene in the absence of the resonance (see Section S4, Supporting Information, for details). The calculated time-resolved  $\Delta R/R$  spectra (Figure 3e) agree well with experimental ones except the slight temporal shift of the  $\Delta R/R$  peak with increasing wavelength, which is the result of light dispersion in the optical elements of the experimental setup. The transient reflectance modulation for the bare PC sample is not observed, thus the modulation amplitude in this case is at least two orders of magnitude less than for the sample covered by graphene monolayer. The typical  $\Delta R/R$  values for a bare graphene are found from literature to be change in a wide range from 0.01% to 0.1%.<sup>[10,11]</sup> The calculated value for our experimental parameters is about 0.04% (see Section S6, Supporting Information). Thus, the BSW excitation leads to an enhancement in the ultrafast reflectance modulation in the graphene monolayer by one order of magnitude.

Figure 3f shows the transient reflectance of the sample at the BSW resonance wavelength. After the increase in reflectance during the pump pulse, the correlation of which with the probe pulse is shown by the gray bar, a picosecond relaxation is observed for both TE and TM cases. The pump impact leads to a modulation in the optical constants of graphene. However, in dielectric materials, the change is mainly governed by the optical Kerr effect and occurs only during the femtosecond pump pulse. Thus, the temporal evolution observed in the experiment at longer timescale is largely determined by the processes occurring in the graphene monolayer. There are three main processes in graphene with different timescales. The initial stage corresponding to the increase in reflectance is characterized by the generation of photoexcited electrons together with the electron–electron scattering, which leads to ultrafast thermalization of the electronic subsystem within several tens of femtoseconds establishing hot Fermi–Dirac distribution of electrons.<sup>[40–43]</sup> Then, this distribution cools down via emission of optical phonons within approximately from 100 to 200 fs,<sup>[44–46]</sup> resulting in the hot optical phonon population. Finally, the hot phonons subsequently decay into acoustic modes in a picosecond time scale.<sup>[47,48]</sup> The time constants of the last two processes strongly depend on the substrate and fabrication procedures of graphene and can be found from the biexponential approximation of  $\Delta R/R$  relaxation. We determined fast  $\tau_1 = 130$  fs and slow  $\tau_2 = 0.8$  ps constants to be very close to that reported in previous works.<sup>[10,47]</sup>

The simulation of time-resolved spectra is performed by splitting the time scale into 50-fs segments. The reflectance spectrum of the PC/graphene sample is calculated for each segment using transfer matrix technique<sup>[39]</sup> with stationary values of the refractive indexes of the materials. The time evolution of the reflectance is governed by the time dependence of the graphene complex refractive index  $n(t) + ik(t)$ . The relaxation part of transient reflectance is taken in the following form:

$$n(t) = n_0 + \frac{n_2 I_{\max}}{2} \left( e^{-\frac{t-t_0}{\tau_1}} + e^{-\frac{t-t_0}{\tau_2}} \right) \quad (1)$$

where  $n_0$  is the real part of the unperturbed graphene refractive index,<sup>[38]</sup>  $I_{\max}$  is an experimental peak intensity of the pump radiation,  $t_0 = 200$  fs is time delay corresponding to the maximum of  $\Delta R/R$ , and  $n_2$  is an effective nonlinear refrac-

tive index taken from ref. [49]. The same time dependence is chosen for the imaginary part  $k(t)$  of the refractive index with the unperturbed value  $k_0$  from ref. [38], and  $k_2$  from ref. [49]. The initial part of transient reflectance from 0-fs to 200-fs time delay cannot be interpreted due to insufficient temporal resolution of the measurements. We thus simply approximate the time dependence of the graphene complex refractive index with a linear function for these delays.

The results of calculations are shown in Figures 3b,e and in 3c,f demonstrating excellent agreement with experimental data. Surprisingly, the calculated maximum  $\Delta R/R$  value exactly coincides with experimental one despite the fact that the values of  $n_2$  and  $k_2$  are obtained in previous work<sup>[49]</sup> by z-scan method. This means that significant contribution to these nonlinear coefficients is made by nonparametric processes of generation and scattering of photoexcited electrons, which occur in graphene during the 100-fs pulses used in ref. [49]. The calculations also show, together with experiment, that the maximum modulation of reflection is observed at the wavelength very close to the BSW resonance. We found that the enhanced modulation in reflection is largely caused by the change in the imaginary part of the graphene refractive index, which leads to the decrease in the BSW resonance depth and its blue-shift compensating for the red-shift due to the change in the real part of the refractive index (see Section S5, Supporting Information). For the case of graphene on the substrate without PC, the calculated maximum modulation value is  $-0.04\%$  (see Section S6, Supporting Information). Thus, the high sensitivity of BSW to the optical constants of the monolayer covering the PC leads to an increase in the all-optical modulation of the graphene/PC reflection by an order of magnitude, while maintaining the time evolution of the graphene response. The modulation value obtained in the experiment can be increased by using plane wave illumination to avoid the Q-factor reduction. The respective simulations (see Section S7, Supporting Information) give the modulation value of approximately 3%. We also note that 0.3% modulation is obtained at a pump fluence of only  $40 \mu\text{J cm}^{-2}$  (peak intensity is about  $1 \text{ GW cm}^{-2}$ ), one to two orders of magnitude lower than the damage threshold of graphene.<sup>[50,51]</sup> Thus, even in the system under study, switching values of more than 3% can be expected as the pump fluence approaches the threshold value.

We also measured the temporal integrated reflectance modulation collecting the probe signal at all wavelengths of the laser pulse to check the dependence of modulation on pump fluence. The maxima of normalized transient reflectance for various pump fluences are shown in Figure 4a. Despite the fact that the spectral dependence of the reflection coefficient modulation has regions with both positive and negative modulation values, the integral value of the modulation turns out to be non-zero, but an order of magnitude smaller than the value at the BSW resonant wavelength. We measured the dependence twice, with increasing and decreasing pump fluence, to check additionally the integrity of graphene. The values for particular points are close to each other for increasing and decreasing pump fluence. The transient dependences for these points (Figure 4b) are also similar. This means that no damage to graphene was observed in our experiment. The observed effect allows us to quickly estimate the temporal dynamics of the reflectance modulation without using spectral decomposition.

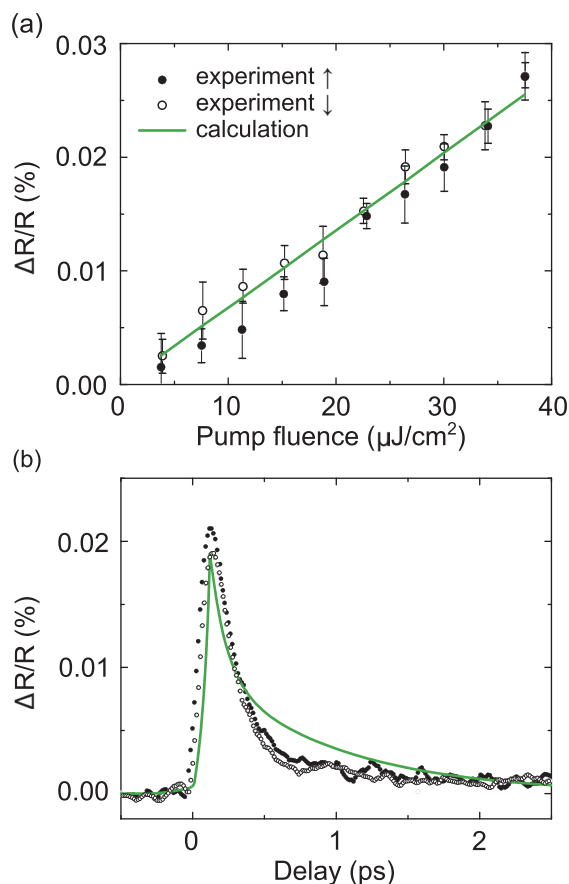


**Figure 4.** a) The dependence of the maxima of normalized transient reflectance of PC/graphene sample on the pump fluence for increasing (filled circles) and decreasing (open circles) pump power and the results of numerical calculations (green line). b) Normalized transient reflection of probe pulses measured for 30  $\mu\text{J}/\text{cm}^2$  pump.

### 3. Conclusion

In conclusion, Bloch surface waves excited at PC/graphene interface enhance significantly the magnitude of ultrafast reflectance modulation. The resonance wavelengths are governed by photonic crystal parameters and can be easily tuned to the desired spectral range. Using the pump-probe technique, we have shown that the magnitude of the reflectance modulation is approximately 10 times larger than that for the bare graphene monolayer, while the temporal dynamics is determined by graphene. The resulting amplitude of reflection modulation is limited due to the large absorption in the graphene monolayer, which leads to a considerable decrease in the Q-factor of the surface wave resonance. To get closer to the values more suitable for applications, it is advisable to consider 2D materials and thin films with high third-order optical susceptibility in spectral regions of their transparency (possible options are transition metal dichalcogenides or hexagonal boron nitride). The low absorption in the vicinity of the BSW resonance should retain the high Q-factor of the mode, which in turn significantly increases the sensitivity of the scheme to the optical parameters of the nonlinear layer and thus the all-optical reflection

modulation. The reported results is a proof of principle possibility of amplifying the reflection modulation of graphene and other nonlinear materials by means of BSW excitation.

### 4. Experimental Section

Experimental samples were distributed Bragg reflectors formed by 7 pairs of quarter-wavelength-layers with thicknesses of 160 and 112 nm for  $\text{SiO}_2$  and  $\text{Ta}_2\text{O}_5$ , respectively, fabricated by physical vapor deposition (PVD). Additional 260 nm-thick layer of  $\text{SiO}_2$  was sputtered on top of PC. These parameters were chosen to excite BSW at approximately 800 nm wavelength of the laser pulses for the incident angle of  $45^\circ$ . The surface of PC was covered with a graphene monolayer prepared by chemical vapor deposition method (CVD) and transferred to sample using wet transfer by polymethyl methacrylate.

### Supporting Information

Supporting Information is available from the Wiley Online Library or from the author.

### Acknowledgements

This work was performed under partial financial support of the Russian Ministry of Education and Science (Grant No. 14.W03.31.0008), Russian Science Foundation (Grant No. 20-12-00371). Part of the research was supported by MSU Quantum Technology Centre and the Development program of the MSU Interdisciplinary Scientific and Educational School "Photonic and Quantum technologies. Digital medicine." M.G.R. and E.D.O. acknowledge financial support by Russian Foundation for Basic Research (Grant No.18-29-19113). A.A.P. acknowledges support by Foundation for the Advancement of Theoretical Physics and Mathematics "BASIS" (Grant No. 19-2-6-28-1).

### Conflict of Interest

The authors declare no conflict of interest.

### Data Availability Statement

The data that support the findings of this study are available from the corresponding author upon reasonable request.

### Keywords

all-optical switching, Bloch surface waves, graphene, pump-probe technique, temporal dynamics

Received: September 10, 2021  
Revised: November 11, 2021  
Published online: December 20, 2021

- [1] S. Thakur, B. Semnani, S. Safavi-Naeini, A. H. Majedi, *Sci. Rep.* **2019**, *9*, 10540.
- [2] K. S. Novoselov, D. Jiang, F. Schedin, T. Booth, V. Khotkevich, S. Morozov, A. K. Geim, *Proc. Natl. Acad. Sci.* **2005**, *102*, 10451.

- [3] V. N. Kotov, B. Uchoa, V. M. Pereira, F. Guinea, A. C. Neto, *Rev. Mod. Phys.* **2012**, *84*, 1067.
- [4] F. Bonaccorso, Z. Sun, T. Hasan, A. Ferrari, *Nat. Photonics* **2010**, *4*, 611.
- [5] F. Xia, T. Mueller, Y.-m. Lin, A. Valdes-Garcia, P. Avouris, *Nat. Nanotechnol.* **2009**, *4*, 839.
- [6] H. Zhang, D. Tang, L. Zhao, Q. Bao, K. Loh, *Opt. Express* **2009**, *17*, 17630.
- [7] Z. Sun, T. Hasan, F. Torrisi, D. Popa, G. Privitera, F. Wang, F. Bonaccorso, D. M. Basko, A. C. Ferrari, *ACS Nano* **2010**, *4*, 803.
- [8] M. Ponarina, A. Okhromchuk, G. Alagashev, G. Orlova, T. Dolmatov, M. Rybin, E. Obraztsova, V. Bukin, P. Obraztsov, *Appl. Phys. Express* **2021**, *14*, 072001.
- [9] M. Liu, X. Yin, E. Ulin-Avila, B. Geng, T. Zentgraf, L. Ju, F. Wang, X. Zhang, *Nature* **2011**, *474*, 64.
- [10] J. M. Dawlaty, S. Shivaraman, M. Chandrashekar, F. Rana, M. G. Spencer, *Appl. Phys. Lett.* **2008**, *92*, 042116.
- [11] B. A. Ruzicka, S. Wang, J. Liu, K.-P. Loh, J. Z. Wu, H. Zhao, *Opt. Mater. Express* **2012**, *2*, 708.
- [12] A. Molinos-Gómez, M. Maymó, X. Vidal, D. Velasco, J. Martorell, F. López-Calahorra, *Adv. Mater.* **2007**, *19*, 3814.
- [13] A. N. Grigorenko, M. Polini, K. Novoselov, *Nat. Photonics* **2012**, *6*, 749.
- [14] J. D. Cox, F. J. Garcia de Abajo, *ACS Photonics* **2015**, *2*, 306.
- [15] Y. Matyushkin, S. Danilov, M. Moskotin, V. Belosevich, N. Kurova, M. Rybin, E. D. Obraztsova, G. Fedorov, I. Gorbenko, V. Kachorovskii, S. Ganichev, *Nano Lett.* **2020**, *20*, 7296.
- [16] B. I. Afinogenov, V. O. Bessonov, I. V. Soboleva, A. A. Fedyanin, *ACS Photonics* **2019**, *6*, 844.
- [17] A. Yariv, P. Yeh, *Optical Waves in Crystals*, Vol. 5, Wiley, New York **1984**.
- [18] A. Sinibaldi, N. Danz, E. Descrovi, P. Munzert, U. Schulz, F. Sonntag, L. Dominici, F. Michelotti, *Sens. Actuators B Chem.* **2012**, *174*, 292.
- [19] M. Zhang, H. Liu, H. Zhou, J. Xiao, *Opt. Commun.* **2018**, *410*, 479.
- [20] E. Guillermain, V. Lysenko, T. Benyattou, *J. Lumin.* **2006**, *121*, 319.
- [21] A. L. Lereu, M. Zerrad, A. Passian, C. Amra, *Appl. Phys. Lett.* **2017**, *111*, 011107.
- [22] R. Dubey, E. Barakat, M. Häyrynen, M. Roussey, S. K. Honkanen, M. Kuittinen, H. P. Herzig, *J. Eur. Opt. Soc.-Rapid Publ.* **2017**, *13*, 5.
- [23] D. A. Shilkin, E. V. Lyubin, I. V. Soboleva, A. A. Fedyanin, *Opt. Lett.* **2015**, *40*, 4883.
- [24] M. N. Romodina, I. V. Soboleva, A. I. Musorin, Y. Nakamura, M. Inoue, A. A. Fedyanin, *Phys. Rev. B* **2017**, *96*, 081401.
- [25] V. N. Konopsky, E. V. Alieva, S. Y. Alyatkin, A. A. Melnikov, S. V. Chekalin, V. M. Agranovich, *Light Sci. Appl.* **2016**, *5*, e16168.
- [26] E. Descrovi, T. Sfez, M. Quaglio, D. Brunazzo, L. Dominici, F. Michelotti, H. P. Herzig, O. Martin, F. Giorgis, *Nano. Lett.* **2010**, *10*, 2087.
- [27] G. Rodriguez, D. Aurelio, M. Liscidini, S. Weiss, *Appl. Phys. Lett.* **2019**, *115*, 011101.
- [28] K. R. Safronov, D. N. Gulkin, I. M. Antropov, K. A. Abrashitova, V. O. Bessonov, A. A. Fedyanin, *ACS Nano* **2020**, *14*, 10428.
- [29] D. N. Gulkin, A. A. Popkova, B. I. Afinogenov, D. A. Shilkin, K. Kuršelis, B. N. Chichkov, V. O. Bessonov, A. A. Fedyanin, *Nano-photonics* **2021**, *10*, 2939.
- [30] F. Barachati, A. Fieramosca, S. Hafezian, J. Gu, B. Chakraborty, D. Ballarini, L. Martinu, V. Menon, D. Sanvitto, S. Kéna-Cohen, *Nat. Nanotechnol.* **2018**, *13*, 906.
- [31] Q. Yang, C. Zhang, S. Wu, S. Li, Q. Bao, V. Giannini, S. A. Maier, X. Li, *Nano Energy* **2018**, *48*, 161.
- [32] M. G. Rybin, A. S. Pozharov, C. Chevalier, M. Garrigues, C. Seassal, R. Peretti, C. Jamois, P. Viktorovitch, E. D. Obraztsova, *Phys. Status Solidi B* **2012**, *249*, 2530.
- [33] W. Kong, Y. Sun, Y. Lu, *Results Phys.* **2020**, *17*, 103107.
- [34] K. V. Sreekanth, S. Zeng, J. Shang, K.-T. Yong, T. Yu, *Sci. Rep.* **2012**, *2*, 737.
- [35] E. Kretschmann, *Opt. Commun.* **1972**, *6*, 185.
- [36] M. Rybin, A. Pereyaslavtsev, T. Vasilieva, V. Myasnikov, I. Sokolov, A. Pavlova, E. Obraztsova, A. Khomich, V. Ralchenko, E. Obraztsova, *Carbon* **2016**, *96*, 196.
- [37] G. B. Barin, Y. Song, I. de Fátima Gimenez, A. G. Souza Filho, L. S. Barreto, J. Kong, *Carbon* **2015**, *84*, 82.
- [38] B. Song, H. Gu, S. Zhu, H. Jiang, X. Chen, C. Zhang, S. Liu, *Appl. Surf. Sci.* **2018**, *439*, 1079.
- [39] P. Yeh, A. Yariv, C.-S. Hong, *J. Opt. Soc. Am.* **1977**, *67*, 423.
- [40] P. A. Obraztsov, M. G. Rybin, A. V. Tyurnina, S. V. Garnov, E. D. Obraztsova, A. N. Obraztsov, Y. P. Svirko, *Nano Lett.* **2011**, *11*, 1540.
- [41] D. Brida, A. Tomadin, C. Manzoni, Y. J. Kim, A. Lombardo, S. Milana, R. R. Nair, K. S. Novoselov, A. C. Ferrari, G. Cerullo, *Nat. Commun.* **2013**, *4*, 1987.
- [42] E. Malic, T. Winzer, E. Bobkin, A. Knorr, *Phys. Rev. B* **2011**, *84*, 205406.
- [43] M. Breusing, S. Kuehn, T. Winzer, E. Malić, F. Milde, N. Severin, J. Rabe, C. Ropers, A. Knorr, T. Elsaesser, *Phys. Rev. B* **2011**, *83*, 153410.
- [44] I. Gierz, J. C. Petersen, M. Mitrano, C. Cacho, I. E. Turcu, E. Springate, A. Stöhr, A. Köhler, U. Starke, A. Cavalleri, *Nat. Mater.* **2013**, *12*, 1119.
- [45] J. C. Johannsen, S. Ulstrup, F. Cilento, A. Crepaldi, M. Zacchigna, C. Cacho, I. E. Turcu, E. Springate, F. Fromm, C. Roidel, *Phys. Rev. Lett.* **2013**, *111*, 027403.
- [46] I. Gierz, S. Link, U. Starke, A. Cavalleri, *Faraday Discuss.* **2014**, *171*, 311.
- [47] K. Kang, D. Abdula, D. G. Cahill, M. Shim, *Phys. Rev. B* **2010**, *81*, 165405.
- [48] H. Wang, J. H. Strait, P. A. George, S. Shivaraman, V. B. Shields, M. Chandrashekar, J. Hwang, F. Rana, M. G. Spencer, C. S. Ruiz-Vargas, *Appl. Phys. Lett.* **2010**, *96*, 081917.
- [49] W. Chen, G. Wang, S. Qin, C. Wang, J. Fang, J. Qi, X. Zhang, L. Wang, H. Jia, S. Chang, *AIP Adv.* **2013**, *3*, 042123.
- [50] M. Currie, J. D. Caldwell, F. J. Bezares, J. Robinson, T. Anderson, H. Chun, M. Tadjer, *Appl. Phys. Lett.* **2011**, *99*, 211909.
- [51] G. Xing, H. Guo, X. Zhang, T. C. Sum, C. H. A. Huan, *Opt. Express* **2010**, *18*, 4564.